European Spine Journal (2022) 31:882–888
https://doi.org/10.1007/s00586-022-07153-7

ORIGINAL ARTICLE

In vivo detection of the lumbar intraforaminal ligaments by MRI

Jeanette Henkelmann[1] · Dina Wiersbicki[2] · Hanno Steinke[2] · Timm Denecke[1] · Christoph-Eckhard Heyde[3] · Anna Voelker[3]

Received: 29 May 2021 / Revised: 9 January 2022 / Accepted: 13 February 2022 / Published online: 11 March 2022

Abstract

Purpose Intraforaminal ligaments (IFL) are of great interest to anatomists and clinicians to fully understand the detailed anatomy of the neuroforamina and to diagnose unclear radicular symptoms. Studies published until now have described radiological imaging of the IFLs using magnetic resonance imaging (MRI) on donor bodies. In the present study, we investigated the detectability of lumbar IFLs in vivo in adults using the high spatial resolution of the constructive interference in steady state (CISS) sequence.

Methods A total of 14 patients were studied using a 1.5 T MRI scanner. The lumbar spine was imaged using the parasagittal CISS sequence, and the detectability of the IFLs was assessed for each lumbar level. All image datasets were analyzed by a radiologist, an orthopedic surgeon, and an anatomist. Interrater reliability was expressed as Fleiss' Kappa. Using a single data set, a three-dimensional (3D) model was created to map the location of the IFLs within the intervertebral foramen (IF) and the immediate surrounding vessels.

Results Overall, the radiologist was able to detect IFLs in 60% of all imaged IFs, the orthopedic surgeon in 62%, and the anatomist in 66%. Fleiss' Kappa for the various segments varies from 0.71 for L4/5 up to 0.90 for L3/4.

Conclusion Lumbar IFLs were successfully detected in vivo in every patient. The detection frequency varied from 42–86% per IF. We demonstrated reproducible imaging of the IFLs on MRI, with good interrater reliability. The present study was a launching point for further clinical studies investigating the potential impact of altered IFLs on radicular pain.

Keywords Clinical imaging · Magnetic resonance imaging · Lumbar spine · Intraforaminal ligaments · Radicular pain

Introduction

Symptoms in the area of the lumbar spine, such as low back pain and radicular pain, are among the most frequent reasons for consulting with patients in the clinical practice of orthopedics. To improve patient care, a comprehensive examination and thorough knowledge of the anatomical region is necessary. In most cases, radicular pain syndromes can be adequately explained by specific pathologies in the lumbar spine, such as disc herniation and neuroforaminal stenosis. However, patients frequently present with leg pain without a clear explanation in terms of etiology. In addition to spinal nerves, the intervertebral foramen (IF) contains blood vessels, lymphatic vessels, and the intraforaminal ligaments (IFLs). The IFLs divide the neuroforamen into different compartments [1] and function to protect the spinal nerves and connect and attach the spinal nerve to the bone of the IF via the surrounding connective tissue [2]. Hypothetically, thickening of the IFLs can lead to an affection of the spinal nerve in the IF, causing radicular leg pain.

In a previous study, we focused on the anatomy of the lumbar IFLs and their close topographical relationship to the lumbar spinal nerves [3]. According to Lee et al. [4], the IF can be divided into an entrance zone (medial side of the pedicle and superior articular process), a mid-zone (below the pedicle and the pars articular is of the lamina), and an exit zone (surrounding the IF). The IFLs were then

✉ Anna Voelker
anna.voelker@medizin.uni-leipzig.de

[1] Department of Diagnostic and Interventional Radiology, University Hospital Leipzig, Liebigstraße 20, 04103 Leipzig, Germany

[2] Institute of Anatomy, Leipzig University, Liebigstraße. 13, 04103 Leipzig, Germany

[3] Department of Orthopedics, Trauma and Plastic Surgery, University Hospital Leipzig, Liebigstraße 20, 04103 Leipzig, Germany

subdivided to correspond with the anatomical classification of the IF. In the entrance zone of the IF, very thin ligaments course from the dorsal side of the vertebral body and the articular processes to the perineurium of the spinal nerve. More laterally, in the middle zone, thicker ligaments oriented vertically connect the pedicles of adjacent vertebrae, or the back of the vertebral body with the intervertebral disc. Also in the middle zone, the thickest IFLs link the vertebral body and articular processes, or the capsule of the facet joint and the intervertebral disc in a horizontal direction. These ligaments are located more laterally than the vertical ligaments. Calgar et al. [5] were able to detect either y-shaped or simple stranded IFLs in 15 cadavers in the exit zone, which divided this zone into either two or three compartments.

So far, no consensus is reached on the nomenclature of the "foraminal ligaments". Considering Lee's division of the IF, our described ligaments are located in the mid-zone and therefore inside the IF. As a comparison to extraforaminal ligaments, we use the term "intraforaminal ligaments" following our previous study and the current publication of Zhong et al. [6].

The hypothesis that IFLs may play an important role in degenerative or pathological changes has been previously discussed in available literature [7, 8]. To form a more complete anatomical picture of these ligaments relevant to routine clinical practice, several research groups have evaluated the IFLs of donor bodies with correlated medical imaging [9–11]. To better differentiate the IFLs from the surrounding structures in the neuroforamina, preliminary work included high-resolution sectioning techniques combined with modified staining and plastination techniques, which were correlated with computed tomography (CT) and magnetic resonance imaging (MRI) of the same specimens [3]. Conventional T2-weighted (T2W) MRI sequences from human cadavers are most commonly used to visualize the IFLs [10].

The constructive interference in steady state (CISS) sequence is a specialized MRI sequence used primarily in imaging of the brain and spinal cord. A strong T2W three-dimensional (3D) gradient echo technique was used, in which the image contrast is characterized by a high signal for fat and water (e.g., cerebrospinal fluid) at submillimeter spatial resolution. This allows for excellent visualization of small-caliber anatomy, such as nerve roots and ligamentous structures [12].

To date, all studies published involving the medical imaging of the IFLs, including our preliminary work, were based on MRIs of body donors only. To the best of our knowledge, this is the first study to investigate the detectability of lumbar IFLs in vivo in live adults using MRI, by leveraging the excellent spatial resolution of the CISS sequence. These new insights into the structural anatomical details of lumbar IFLs may provide further information for understanding potential pathologies involving this part of the body.

Materials and methods

Study cohorts

This prospective study included adult patients referred to our hospital for MRI for nonspecific lumbar spine pain, with or without associated leg pain. The exclusion criteria were as follows: patients with a history of spinal surgery, lumbar scoliosis, lumbar vertebral fractures, and/or contraindications to MRI (i.e., pacemakers, metallic foreign bodies, or severe claustrophobia).

The Ethics Committee of the Medical Faculty of the University of Leipzig, Germany (009/20-ek) provided approval for the present study in accordance with the 1964 Declaration of HELSINKI and its subsequent amendments. Written informed consent was obtained from each patient prior to undergoing MRI of the lumbar spine.

Magnetic resonance imaging

All unenhanced MRI scans of the lumbar spine for the present study were acquired using a Magnetom Aera 1.5 T MRI scanner (Siemens, Erlangen, Germany) with an integrated spine coil. In addition to the standard protocol of a conventional sagittal T1-weighted turbo spin-echo sequence (T1W-TSE), sagittal, axial, and oblique-coronal T2W-TSE, and parasagittal 3D-CISS sequences were performed. The detectability of the IFLs was evaluated using the acquired CISS image series for each patient. For the present study, we predetermined that only the right-sided neuroforamina of the lumbar spine would be examined with the additional sequences (3D-CISS), as the feasibility of IFL imaging was the primary concern. To accurately depict the anatomical course of the neuroforamen, the oblique-coronal T2W series was first aligned orthogonally with the long axis of the lumbar lordosis as best as possible. The parasagittal 3D-CISS sequence was then aligned using the oblique-coronal and axial T2W images. Figure 1 illustrates the planning of the image slices. Figure 2 shows an example of lumbar IF images created using the CISS sequence. The 3D-CISS sequence used the following parameters: slice thickness, 1 mm; repetition time/echo time (TR/TE), 5.81/2.51 ms; voxel size, 0.3 mm^3; field of view (FOV), 180 mm; flip angle, 70°; and acquisition time, 3 min 59 s.

Image data analysis and post-processing

All images in the 3D-CISS sequences were reviewed in detail for the presence of IFLs by one board-certified radiologist (R) with six years of experience specializing in musculoskeletal imaging, one board-certified orthopedic

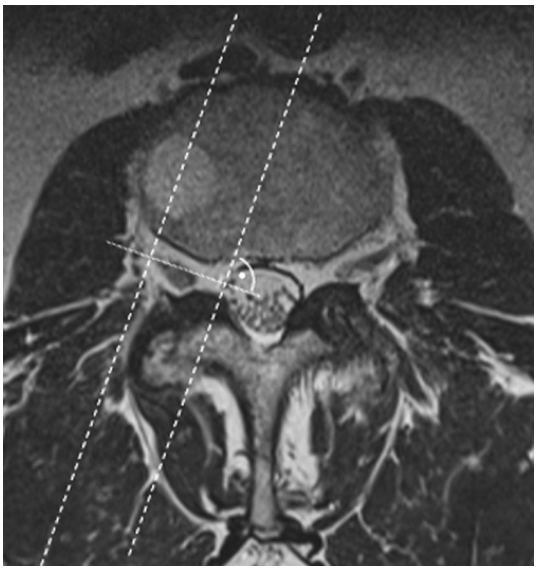

Fig. 1 Axial T2-weighted magnetic resonance imaging (MRI) for planning the parasagittal constructive interference in steady state (CISS) sequence at the level of the nerve root; the slices were aligned perpendicularly to the course of the intervertebral foramen; incidental right paramedian vertebral body hemangiomas

surgeon (O) with seven years of experience specializing in spine surgery, and one anatomist (A) with five years of experience specializing in plastination and with prior scientific knowledge in the clinical imaging of IFLs.

Image analysis was performed using Syngo Plaza software (Siemens Medical Solutions, Germany). First, each of the three evaluators performed training to evaluate the IFLs of 15 patients using CISS sequences, so that they could be reliably identified in the study group. The training data set was not included in the data set of the present study.

The frequency of IFL detection in the study group was assessed by each of the three evaluators for each lumbar level. IFL identification was defined as follows: low-signal, linear structure observed between the exiting spinal roots and moving to the bony edge of the neuroforamen in the usual topography. IFLs were defined as unidentified when the ligaments were not observed between the nerve root and bony boundary of the IF, when their detection was considered unsatisfactory, or when they might be ambiguous.

Statistical analyses

Statistical analyses were performed using SPSS (version 22.0®, Chicago, IL, USA). Continuous variables are presented as means with minimum and maximum values. Fleiss' Kappa was used to assess interrater reliability for the three raters (R, O, and A).

Image segmentation

Using the software Materialize Mimics Innovation Suite 22.0 (Materialize GmbH, Gilching, Germany), a 3D model of the lumbar spine of an exemplary patient (patient 8, a 66-year-old male) was created. The location of the IFLs within the IF, as well as the proximity of the surrounding vessels, are depicted in Fig. 3.

Results

A total of 14 patients (11 men and 3 women) were included in the present study. The mean age was 66 ± 9 years (range, 50–82 years). In 10 patients, the entire lumbar spine (L1-L5) was imaged with MRI. In two patients, the neuroforamen at L1/2 was not imaged due to folding artifacts caused by an FOV that was too small. In two other patients, the IF at L1/2 and L2/3 were not imaged for the same reason.

A total of 50 IFs were evaluated by each rater. Table 1 shows the assessment of the respective lumbar neuroforamina by each rater. IFLs were detected in all of the MR images. In addition to the upper lumbar spine region, which was not imaged, some patients did not show evidence of IFLs in several segments. All raters failed to detect IFLs in the IF at L2/3 in six patients, and also at L3/4 in six patients. In total, seven IFs had inconsistent IFL identification (IFL identified/not identified) by the three raters.

Overall, the radiologist was able to detect IFLs in 60% of the imaged IFs, the orthopedic surgeon in 62%, and the anatomist in 66%. Specific to each IF segment, IFL detectability was 80% for each rater in segment L1/2, 42–50% in L2/3 (O and A 42%, R 50%), 50–57% in L3/4 (R and O 50%, A 57%), and 64–86% in L4/5 (R 64%, O 79%, and A 86%). Fleiss' Kappa for the various segments varied from 0.71 for L4/5 up to 0.90 for L3/4 (Table 2).

Figure 3 shows the 3D reconstruction with the anatomical course of the explored horizontal lumbar IFLs. CISS sequences from a 66-year-old male proband (patient 8) were used for segmentation. IFLs were detected in all IFs from L1/2 to L4/5 in this specific patient. IFLs were located transversely in the middle zone of the IF and spanned from the inferior articular processes to the intervertebral disc below the spinal nerve. Two transverse IFLs were detected in the IF at L2/3 and L3/4, and one transverse IFL was found in L1/2 and L2/3. The venous plexus surrounding the aforementioned structures of the IF was also exemplarily imaged.

Discussion

In the present study, we demonstrated that lumbar IFLs are detectable in vivo in adults on MR images with a total frequency of 42–86% per neuroforamen. Overall, detection of

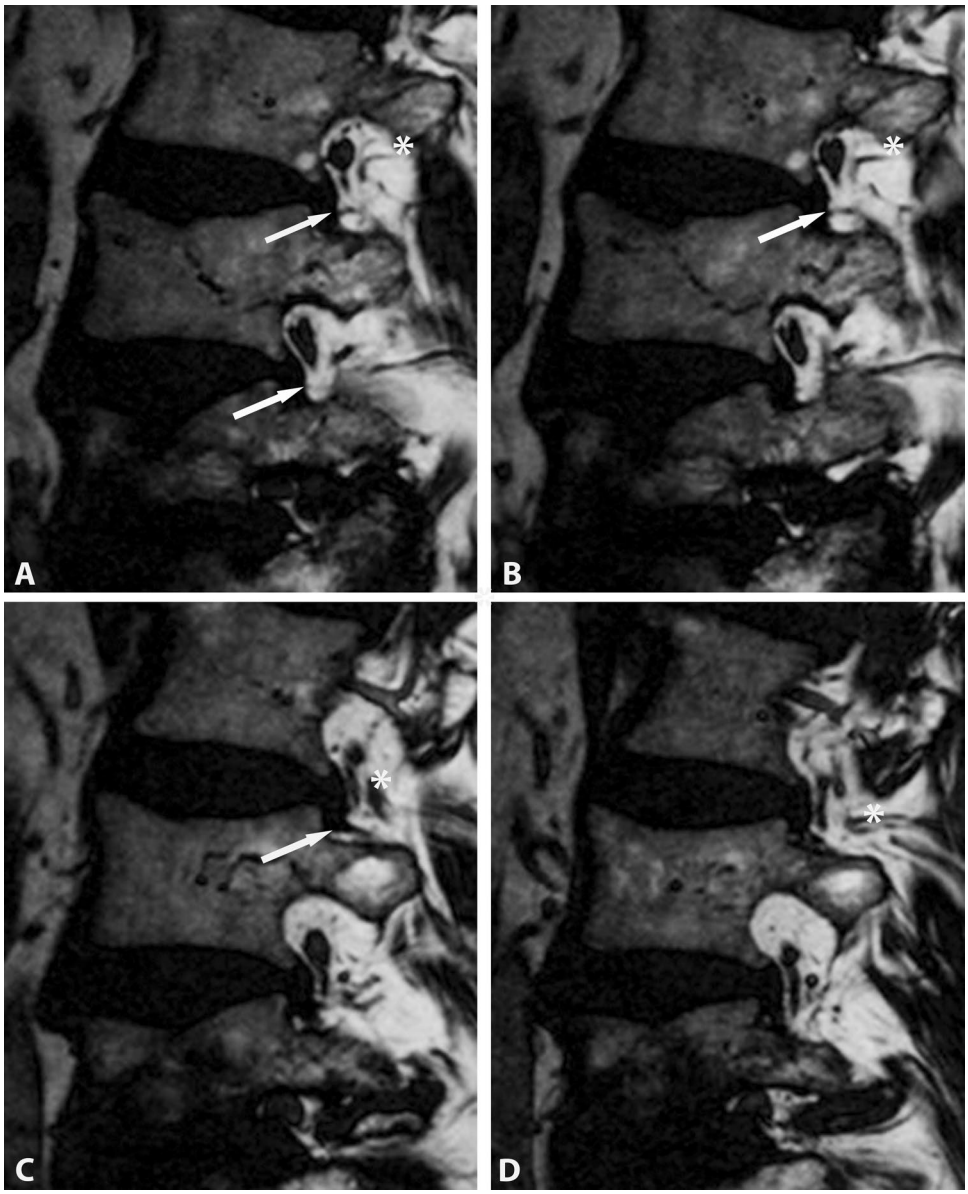

Fig. 2 Sagittal magnetic resonance imaging (MRI) three-dimensional (3D) constructive interference in steady state (CISS) sequence of a 66 year-old male proband: the lumbar spine is seen from the vertebral body L1 to L3; **a** and **b**, as well as **c** and **d**, are consecutive slices; the inferior intervertebral ligament is highlighted with an arrow, and the small vessels are marked with white stars

foraminal ligaments was successful at least at one level in each patient. The available literature shows that IFLs regularly pass through the IF as normal tissue, functioning to attach and protect the spinal nerve and its supporting vessels [1, 13].

In the relevant literature, the percentage of the foraminal ligaments detected in prepared donor bodies varies from 17.8–100%, although the individual preparation methods used to detect IFLs differed between studies [9, 14, 15]. It has been previously reported that most radiologists interpreting MR images in clinical practice do not regularly identify the foraminal bands [10], which is due to the fact that foraminal bands are not yet commonly evaluated due to limited knowledge. Additionally, the detectability of IFLs is a technical challenge, due to it being a small-caliber structure with a reported thickness (diameter) of 0.2–1.5 mm [15]. Achieving high spatial resolution in MRI is also challenging [6]. To cover a large tissue volume, routine axial and sagittal spin echo sequences are typically 3–4-mm-thick, accompanied by high spatial resolution. Imaging technology has advanced significantly and now allows for submillimeter resolutions. Owing to its excellent resolution, the CISS sequence is commonly used for the neuroimaging of small-caliber structures, and many applications of spine imaging using this technique have been discussed [16]. However, CISS sequences must always be interpreted in combination with conventional T1- and T2-weighted images, as they do not promote reliable tissue characterization, but rather provide spatial depiction. It must be noted that the CISS sequence requires additional acquisition time, and time can be a limited resource in MR

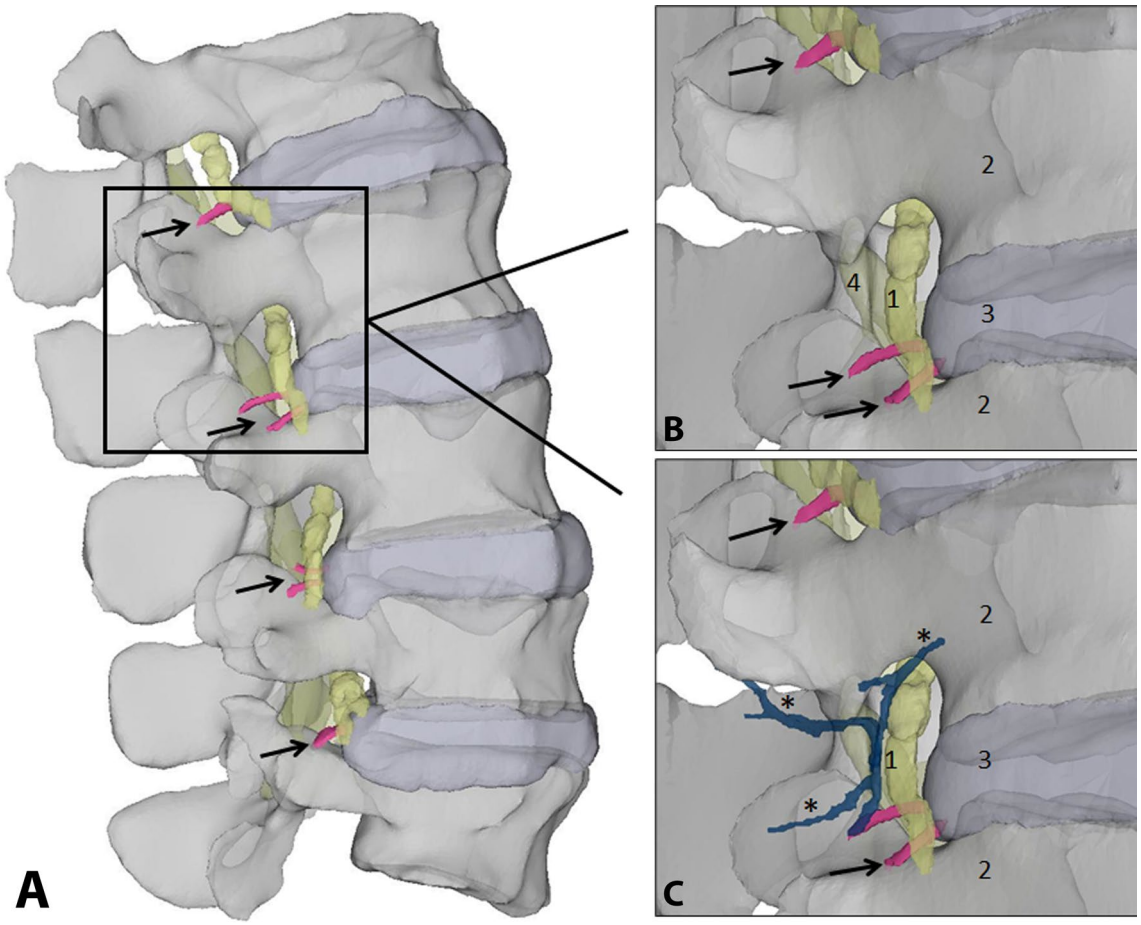

Fig. 3 Three-dimensional (3D) reconstruction of the lumbar spine using the magnetic resonance imaging (MRI) data from the three-dimensional (3D) constructive interference in steady state (CISS) sequence of a 66-year-old male proband, illustrating the anatomical course of the detected intraforaminal ligaments (black arrow) inside the intervertebral foramina: 1—spinal nerve root, 2—vertebral body, 3—intervertebral disc, 4—ligamenta flava; **a** shows a semitransparent overview, in a right lateral view; **b** is a semitransparent lateral close-up of the intervertebral foramina at L2/3; **c** is **a** with additional reconstruction of the small vessels

Table 1 Assessment of detectability the lumbar intraforaminal ligaments by three readers (R, radiologist; O, orthopedic surgeon; A, anatomist; n.i., IFL not imaged; + IFL identified;—IFL not identified)

No	Age	Lumbar level	L1/2			L2/3			L3/4			L4/5		
		Sex	R	O	A	R	O	A	R	O	A	R	O	A
1	72	Male	n.i	n.i	n.i	−	−	−	+	+	+	+	+	+
2	56	Male	+	+	+	+	+	+	−	−	−	+	+	+
3	65	Male	n.i	n.i	n.i	n.i	n.i	n.i	+	+	+	−	+	+
4	82	Male	n.i	n.i	n.i	+	−	−	+	+	+	+	+	+
5	67	Female	+	+	−	−	−	−	−	−	−	−	−	+
6	50	Female	−	−	−	−	−	−	−	−	−	−	+	+
7	72	Male	n.i	n.i	n.i	n.i	n.i	n.i	+	+	+	+	+	+
8	66	Male	+	+	+	+	+	+	+	+	+	+	+	+
9	63	Male	+	+	+	−	−	−	+	+	+	−	−	−
10	54	Male	+	+	+	−	−	−	−	−	−	+	+	+
11	78	Male	+	+	+	−	−	−	−	−	−	+	+	+
12	75	Male	−	−	+	+	+	+	+	+	+	+	+	+
13	69	Female	+	+	+	+	+	+	−	−	+	+	+	+
14	54	Male	+	+	+	+	+	+	−	−	−	−	−	−

Table 2 Shown are the "Fleiss-Kappa" values of the identified or not identified IFL in each single segment of the lumbar spine by radiologist, orthopedic surgeon, and anatomist

Lumbar level	Radiologist		Orthopedic surgeon		Anatomist		Fleiss- Kappa [95% CI]
	Identified	Not identified	Identified	Not identified	Identified	Not identified	
L1/2	8	2	8	2	8	2	0,73 [0.38 – 1]
L2/3	6	6	5	7	5	7	0,79 [0.52 – 1]
L3/4	7	7	7	7	8	6	0,90 [0.72 – 1]
L4/5	9	5	11	3	12	2	0.71 [0,42 – 1]

imaging. Unfortunately, the risk of motion artifacts may increase when performing this additional sequence, due to the longer examination time.

In the present study, we identified the most frequently detected ligamentous structure in the IF as the inferior horizontal ligament (Fig. 3). However, we must note that we did not explicitly classify the detected IFLs in the present study. The IFLs were classified based on their localization from a single subject's dataset, specifically for the segmentation and illustration seen in Fig. 3.

As reported by Park et al. [7], as in the present study, IFLs could not be detected in all IFs of the lumbar spine. In the presence of segmental degenerative changes of a single lumbar segment, narrowing of the IF by intervertebral disc tissue or hypertrophied ligamentum flavum, may occur, especially under axial load [11]. Additionally, hypertrophy of the facet joints can also lead to IF stenosis. During the reduction of the foraminal dimension, all the structures passing through the IF could be compressed [17], which may explain why IFLs were not detectable in all of the imaged IFs. For this reason, we deliberately did not pre-select patients for realistic imaging of a typical patient with spinal disorders.

In addition to the difficulty detecting IFLs due to their small size, there is also a risk that an untrained examiner may misinterpret parts of the intraforaminal vascular plexus as a ligamentous structure on MRI. Detection and interpretation of these complex structures on MRI images requires some training. There was also some variation in detectability in our study. In our interrater evaluation, IFL were most frequently identified by the anatomist. However, all three readers were able to detect the IFL reproducibly, ultimately with some variation that statistically resulted in a good interrater reliability.

The spinal nerve comprises 10–30% of the total cross-sectional area of the IF [18]. Despite the large residual space around the spinal nerve, it is conceivable that, in addition to extraforaminal degenerative changes, hypertrophy of the IFLs may potentially lead to spinal nerve affection.

Classification of IFLs on MRI images into normal and pathologic IFLs was not subject of the current study but will be necessary in further investigations. Hypothetically, radicular symptoms without evidence of typical disc herniation or IF stenosis due to segmental degeneration but clearly pathologically thickened IFL could lead to nerve root infiltration therapy or surgical decompression of the affected nerve in the corresponding neuroforamen.

In an anatomical study of four cadavers, Grimmes et al. [12] described ligaments in the IF regions of L2/3, L3/4, and L4/5, stating that these IFLs increase in thickness and width from cranial to caudal segments. This phenomenon may explain why IFLs were most frequently detected in the L4/5 segment on MR images in the present study.

Conclusion

IFLs are components of the neuroforamen, which function to attach the spinal nerve to the bony canal. Specialized MRI sequences, such as the high-resolution 3D-CISS sequence, can reliably detect IFLs in MR images, with the trained examiner able to easily identify IFLs. In the present study, we demonstrated reproducible imaging-based identification of the IFLs on MRI, with good interrater reliability. The accurate and reliable identification of IFLs is necessary for further clinical studies to investigate the possible influence of altered IFLs on radicular pain.

Acknowledgements The authors are thankful to Heike Röder for providing the MR images from the Department of Diagnostic and Interventional Radiology, University Hospital Leipzig.

Funding Open Access funding enabled and organized by Projekt DEAL. Not applicable.

Data availability All relevant data generated or analyzed during the current study are presented in this paper.

Declarations

Conflict of interest The authors have no conflicts of interest to declare.

Ethical approval All procedures in the present study involving human participants were performed in accordance with the ethical standards of the institutional research committee (Ethics Committee of the Medical Faculty at the University of Leipzig, Germany; 009/20-ek) and

with the 1964 Declaration of HELSINKI and its later amendments, or comparable ethical standards.

Consent to participate Informed consent was obtained from all participants included in the study.

Consent for publication All authors consent to the publication of the manuscript.

References

1. Yuan S-G, Wen Y-L, Zhang P et al (2015) Ligament, nerve, and blood vessel anatomy of the lateral zone of the lumbar intervertebral foramina. Int Orthop 39:2135–2141. https://doi.org/10.1007/s00264-015-2831-6
2. Wiltse LL (2000) Anatomy of the extradural compartments of the lumbar spinal canal. Peridural membrane and circumneural sheath. Radiol Clin North Am 38:1177–1206. https://doi.org/10.1016/s0033-8389(08)70003-4
3. Wiersbicki D, Völker A, Heyde C-E et al (2019) Ligamental compartments and their relation to the passing spinal nerves are detectable with MRI inside the lumbar neural foramina. Eur Spine J 28:1811–1820. https://doi.org/10.1007/s00586-019-06024-y
4. Lee CK, Rauschning W, Glenn W (1988) Lateral lumbar spinal canal stenosis: classification, pathologic anatomy and surgical decompression. Spine 13:313–320. https://doi.org/10.1097/00007632-198803000-00015
5. Caglar YYS, Dolgun H, Ugur HC et al (2004) A ligament in the lumbar foramina: inverted Y ligament: an anatomic report. Spine 29:1504–1507. https://doi.org/10.1097/01.brs.0000131437.86606.63
6. Zhong E, Zhao Q, Shi B et al (2018) The morphology and possible clinical significance of the intraforaminal ligaments in the entrance zones of the L1–L5 Levels. Pain Physician 21:E157–E165
7. Park HK, Rudrappa S, Dujovny M et al (2001) Intervertebral foraminal ligaments of the lumbar spine: anatomy and biomechanics. Childs Nerv Syst 17:275–282. https://doi.org/10.1007/pl00013729
8. Qian Y, Qin A, Zheng MH (2011) Transforaminal ligament may play a role in lumbar nerve root compression of foraminal stenosis. Med Hypotheses 77:1148–1149. https://doi.org/10.1016/j.mehy.2011.09.025
9. Cramer GD, Skogsbergh DR, Bakkum BW et al (2002) Evaluation of transforaminal ligaments by magnetic resonance imaging. J Manip Physiol Ther 25:199–208. https://doi.org/10.1067/mmt.2002.123174
10. Marić DL, Krstonošić B, Erić M et al (2015) An anatomical study of the lumbar external foraminal ligaments: appearance at MR imaging. Surg Radiol Anat 37:87–91. https://doi.org/10.1007/s00276-014-1320-8
11. Nowicki BH, Haughton VM, Schmidt TA et al (1996) Occult lumbar lateral spinal stenosis in neural foramina subjected to physiologic loading. AJNR Am J Neuroradiol 17:1605–1614
12. Ramli N, Cooper A, Jaspan T (2001) High resolution CISS imaging of the spine. Br J Radiol 74:862–873. https://doi.org/10.1259/bjr.74.885.740862
13. Grimes PF, Massie JB, Garfin SR (2000) Anatomic and biomechanical analysis of the lower lumbar foraminal ligaments. Spine 25:2009–2014. https://doi.org/10.1097/00007632-200008150-00002
14. Golub BS, Silverman B (1969) Transforaminal ligaments of the lumbar spine. J Bone Joint Surg Am 51:947–956
15. Nowicki BH, Haughton VM (1992) Neural foraminal ligaments of the lumbar spine: appearance at CT and MR imaging. Radiology 183:257–264. https://doi.org/10.1148/radiology.183.1.1549683
16. Li Z, Chen YA, Chow D et al (2019) Practical applications of CISS MRI in spine imaging. Eur J Radiol Open 6:231–242. https://doi.org/10.1016/j.ejro.2019.06.001
17. Cinotti G, Santis P, de Nofroni I et al (2002) Stenosis of lumbar intervertebral foramen: anatomic study on predisposing factors. Spine 27:223–229. https://doi.org/10.1097/00007632-200202010-00002
18. Hoyland JA, Freemont AJ, Jayson MI (1989) Intervertebral foramen venous obstruction. A cause of periradicular fibrosis? Spine 14:558–568. https://doi.org/10.1097/00007632-198906000-00002